Supplementary Figures

Figure S1

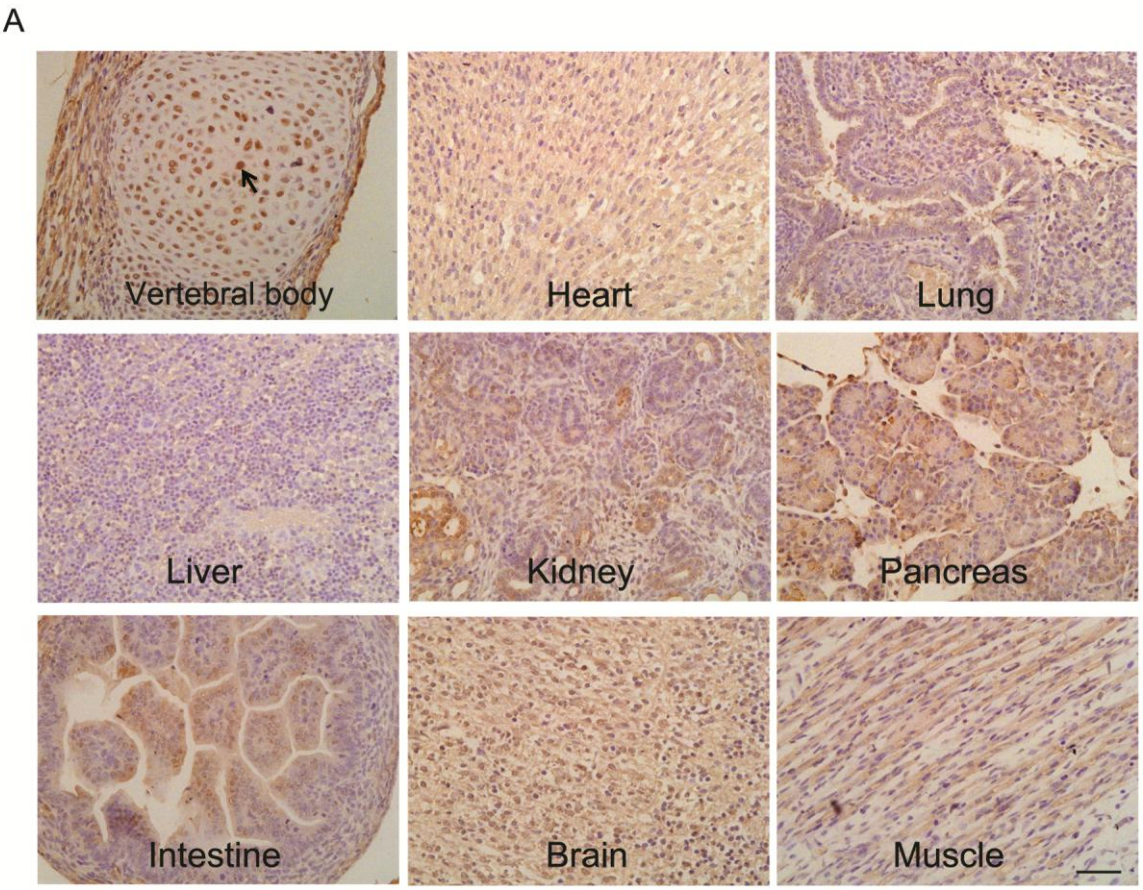

Supplementary Figure S1. JMJD3 is highly expressed in chondrocytes.

(A) Immunohistochemistry with specific anti-JMJD3 antibody at the longitudinal sections of E16.5 mice. The representative magnified images, such as vertebral body, heart, lung, liver, kidney, pancreas, intestine, brain and muscle were showed. The JMJD3 positive nuclei are brown. Black arrow: JMJD3 possitive chondrocyte. Scale bar: 50μm.

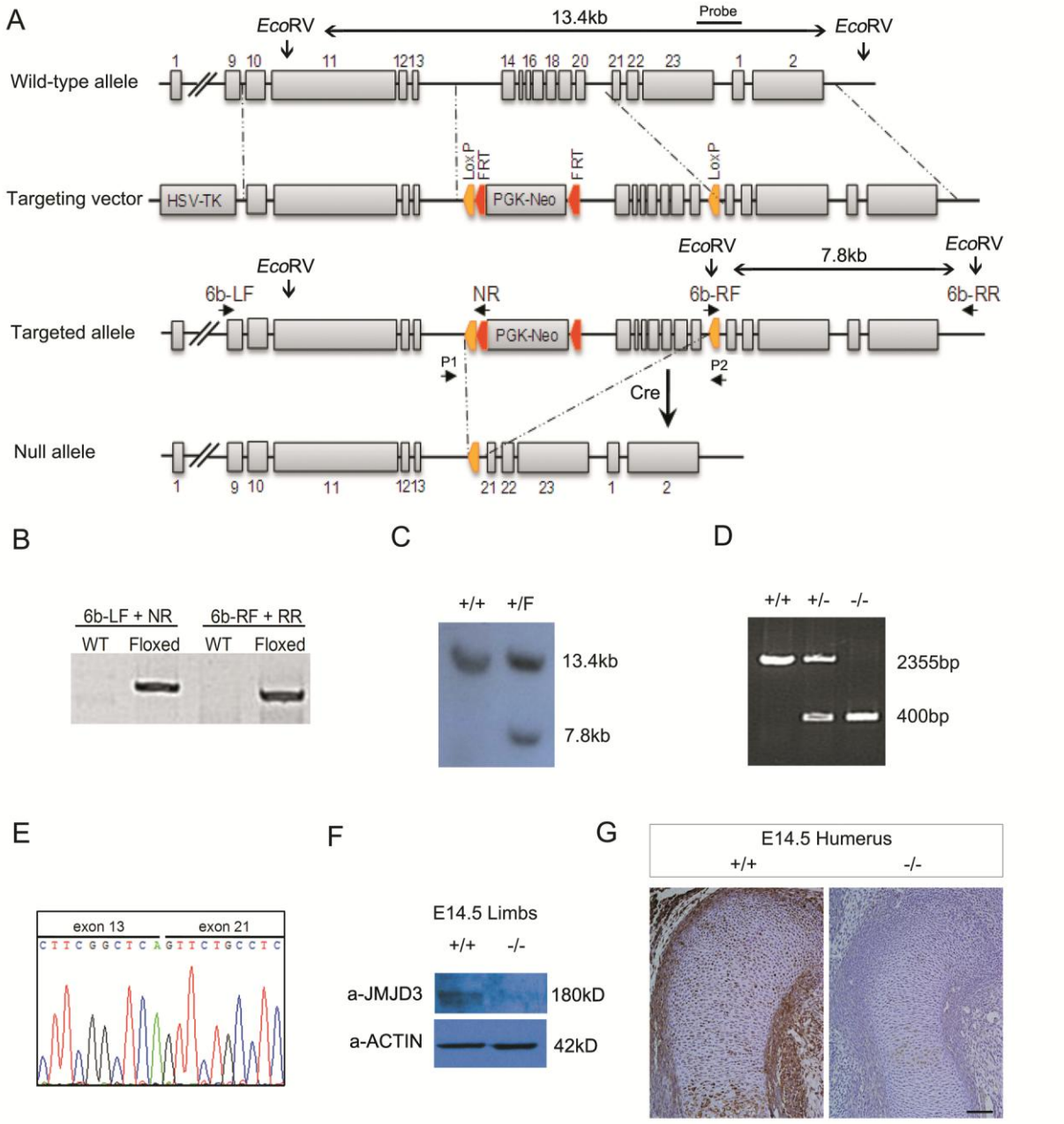

Supplementary Figure S2. Generation of *Jmjd3*$^{-/-}$ mice.

(A) Schematic representation of the *Jmjd3* gene, the targeting vector, targeted allele and the null allele. A targeting vector was designed to replace exon14-20 containing the JmjC H3K27 demethylase domain with a neomycin-resistance gene.

(B) Flox positive ES clone was examined by PCR using primers as indicated above.

(C) Southern blot of genomic DNA extracted from ES cells. Genomic DNA was digested with *Eco*RV, separated by electrophoresis and hybridized with the radiolabelled probe as indicated. A southern blot gave a single band for wild-type (13.4kb) and both bands for *Jmjd3* heterozygous (13.4kb and 7.8kb).

(D) Genotyping of embryos by PCR with primers P1 and P2 as indicated. The fragments indicates the wild-type (2355 bp), heterozygous (2355bp and 400bp) and homozygous (400bp) *Jmjd3* alleles.

(E) The deletion of exons from 14 to 20 was confirmed by cDNA sequencing from $Jmjd3^{-/-}$ mice.

(F) Western blot analysis of JMJD3 expression in limbs of wild-type and homozygous mutant mice at E14.5. β-ACTIN serves as loading control.

(G) Immunohistochemistry of JMJD3 at the humerus longitudinal sections of wild-type and homozygous mutant mice at E14.5. Scale bar: 100μm.

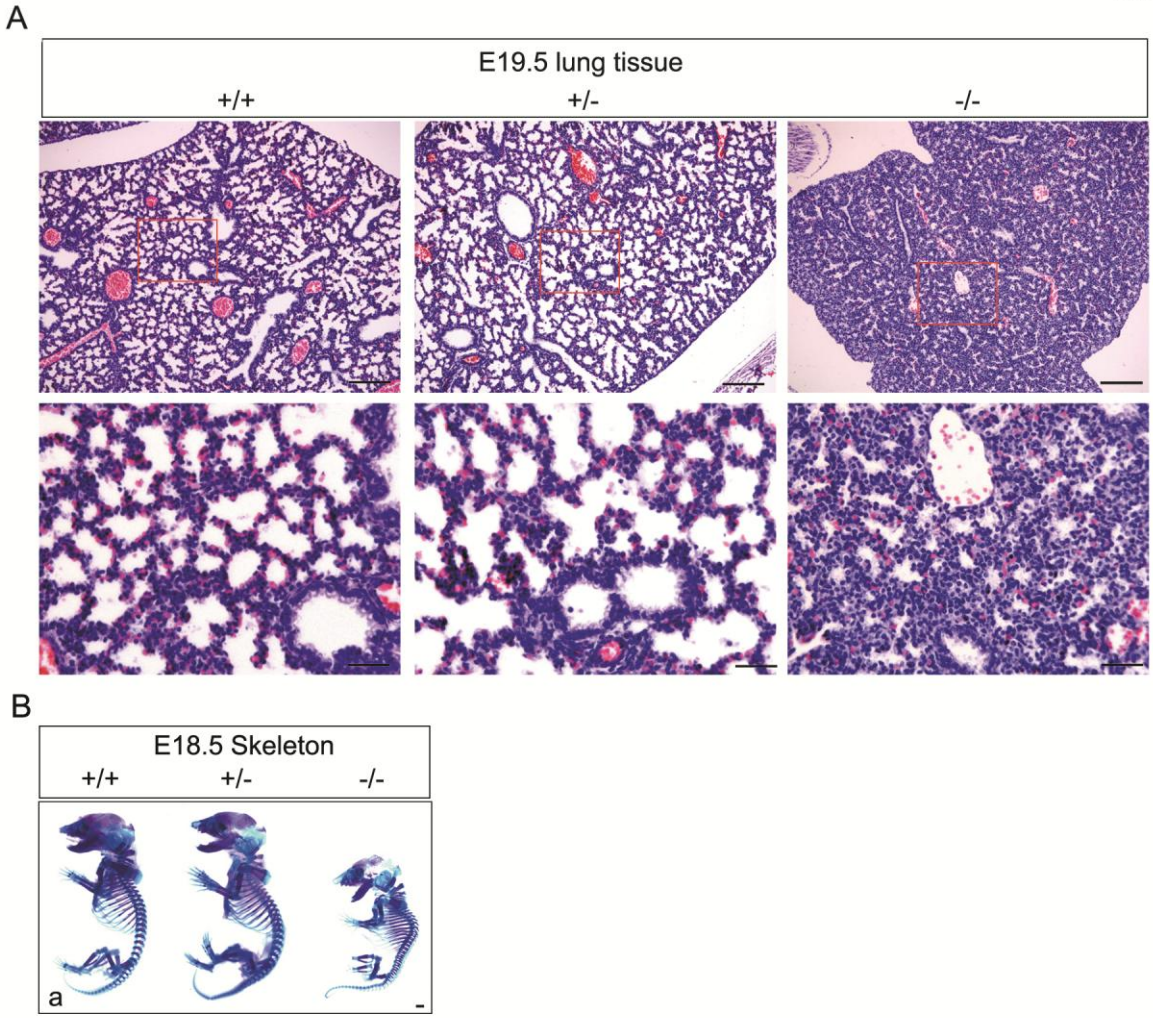

Supplementary Figure S3. Developmental defects of lung and skeleton in *Jmjd3*$^{-/-}$ mice.

(A) H&E staining sections of *Jmjd3*$^{+/+}$, *Jmjd3*$^{+/-}$ and *Jmjd3*$^{-/-}$ lung tissues at E19.5. The boxed regions are magnified beneath respectively. Scale bar: 200μm in panel above and 50μm in panel below.

(B) Skeletons of *Jmjd3*$^{+/+}$, *Jmjd3*$^{+/-}$ and *Jmjd3*$^{-/-}$ embryos at E18.5. Scale bar: 1mm.

Figure S4

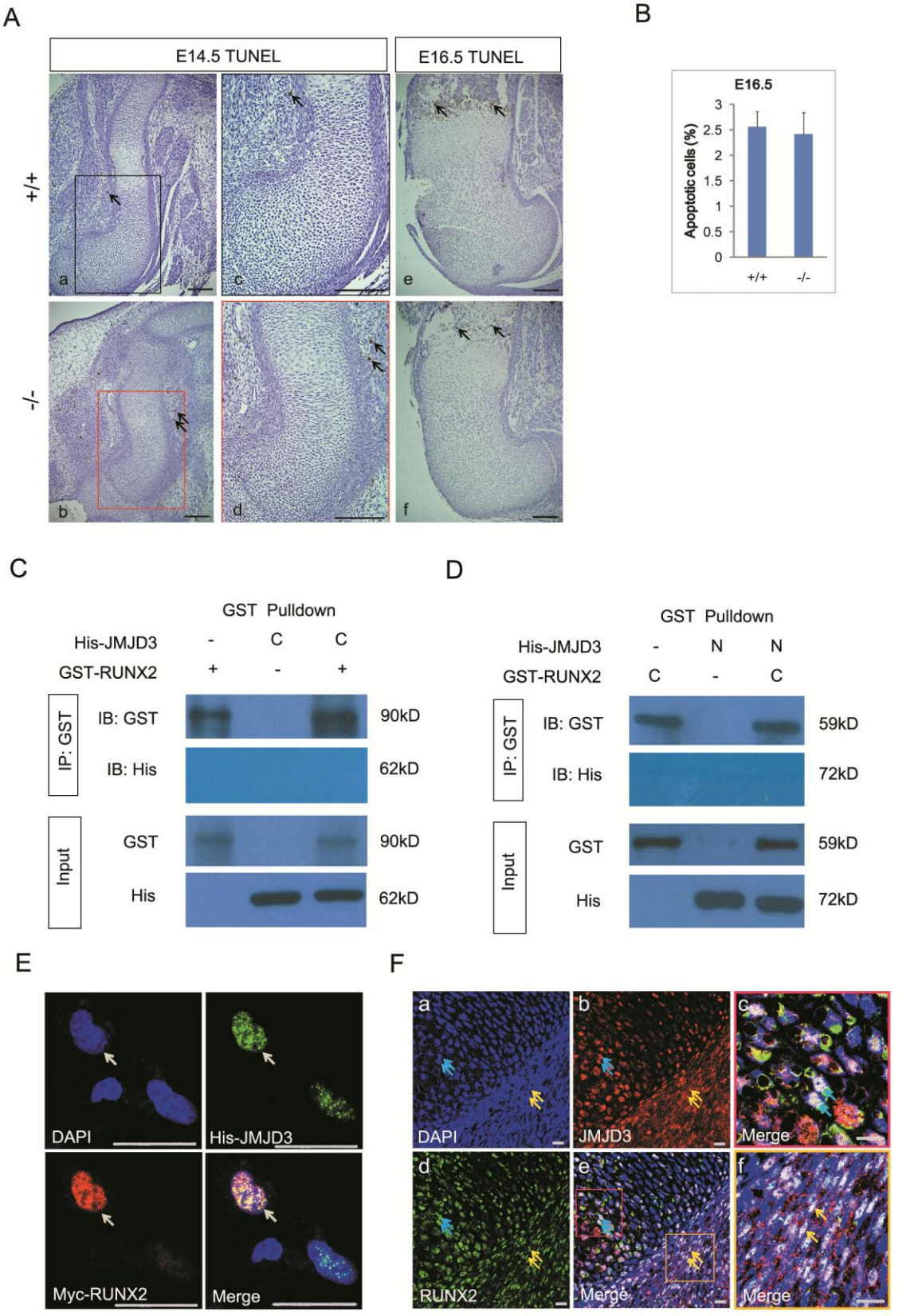
A
E14.5 TUNEL
E16.5 TUNEL
+/+
-/-
a
b
c
d
e
f
B
E16.5
Apoptotic cells (%)
3
2.5
2
1.5
1
0.5
0
+/+
-/-
C
GST Pulldown
His-JMJD3 - C C
GST-RUNX2 + - +
IP: GST
IB: GST
90kD
IB: His
62kD
Input
GST
90kD
His
62kD
D
GST Pulldown
His-JMJD3 - N N
GST-RUNX2 C - C
IP: GST
IB: GST
59kD
IB: His
72kD
Input
GST
59kD
His
72kD
E
DAPI
His-JMJD3
Myc-RUNX2
Merge
F
a
b
c
DAPI
JMJD3
Merge
d
e
f
RUNX2
Merge
Merge

Supplementary Figure. S4. Apoptosis analysis in *Jmjd3*$^{-/-}$ mice and GST-pulldown assays to test JMJD3 interacting with RUNX2

(A) TUNEL assays in humeri sections of WT and *Jmjd3*$^{-/-}$ embryos at E14.5 and E16.5. No apoptotic chondrocyte was detected in the growth plate at E14.5. Apoptotic chondrocytes were primarily detected in the terminal hypertrophic zone of the growth plates at E16.5. The boxed regions in a and b are magnified in c and d with matched color rim respectively. Arrows: TUNEL-positive cells. Scale bar: 200μm.

(B) Quantification of apoptosis rate in chondrocytes represented by the ratio of TUNEL-positive cells normalized to total cells in WT and *Jmjd3*$^{-/-}$ humeri sections at E16.5. Two-tailed Student's t-test. Error bar indicates the SE. n=3.

(C) GST pull-down assays with bacterially expressed GST-RUNX2 and in vitro transcribed/translated JMJD3-C as indicated. No direct interaction was detected between RUNX2 and JMJD3-C.

(D) GST pulldown assays of in vitro transcribed/translated His-JMJD3-N by purified GST-RUNX2-C. No direct interaction was detected between RUNX2-C and JMJD3-N.

(E) Immunofluorescence under confocal microscope with anti-Flag (green) and anti-Myc (Red) antibodies in HEK293T cells, which were cotransfected with Flag-tagged *Jmjd3* and His-Myc-tagged *Runx2*. Arrow denotes that JMJD3 colocalized with RUNX2 in the nuclei of HEK293T cells. Scale bar: 40μm.

(F) Immunofluorescence under confocal microscope with anti-RUNX2 (green)

and anti-JMJD3 (red) antibodies at the section of E14.5 tibia. The zone of prehypertrophic chondrocytes (red box region) and perichondral osteoblasts (orange box region) are magnified at the right with matched color rim respectively. JMJD3 colocalizes with RUNX2 in the nuclei of prehypotrophic chondrocytes (e, c; blue arrows) and perichondral osteoblasts (e, f; orange arrows). Scale bar: 20μm.

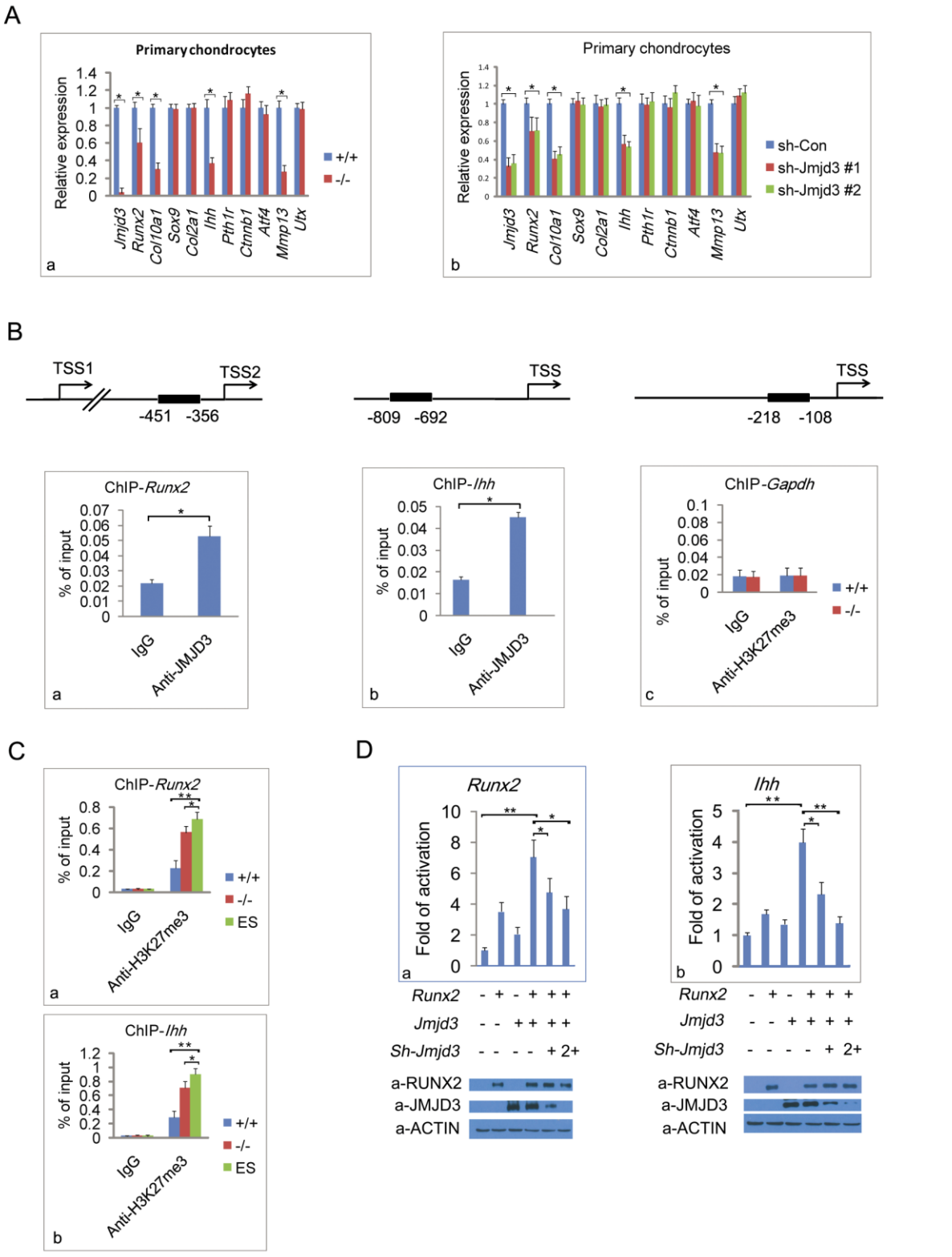

Supplementary Figure S5. Assessment of JMJD3 binding to the promoters of *Runx2* and *Ihh* genes.

(A) Expression levels of chondrocyte-specific genes relative to *Gapdh* in WT and *Jmjd3*$^{-/-}$ limb primary cultured chondrocytes (a) or *Jmjd3* knockdown primary cultured chondrocytes (b) of E14.5 embryos were analyzed by RT-qPCR assays.

(B) JMJD3 occupancies at the *Runx2* (a) *or Ihh* (b) promoter in ATDC5 chondrocytes were detected by ChIP-qPCR investigation. No H3K27me3 was detected at the promoter of *Gapdh* (c) in chondrocytes by ChIP-qPCR assays. Signals are shown as a percentage of the input. The black areas in the schematic promoters of *Runx2* (a), *Ihh* (b) *and Gapdh* (c) are the targeting positions of ChIP-qPCR primers.

(C) H3K27me3 level at the *Runx2* (a) *or Ihh* (b) promoter in embryonic stem (ES) cells, WT and *Jmjd3*$^{-/-}$ primary chondrocytes were investigated by ChIP-qPCR. Signals are shown as a percentage of the input.

(D) Luciferase reporter assays. HEK293 cells were transfected with the pGL3-basic reporter containing 2kb *Runx2* promoter (a) or a 2kb *Ihh* promoter (b) with or without expression plasmids encoding *Runx2* (100 ng) , *Jmjd3* (100 ng) or *Jmjd3*-shRNA (sh-*Jmjd3*) in increasing amounts (50, 100 ng) as indicated. The basal luciferase activity for each reporter was calculated as 1 in y axis. Western blot showing level of expressed proteins in the lysates of transfected cells (bottom).

The above experiments were repeated 3 times. *: $p<0.05$, **: $p<0.01$, Two-tailed Student's t-test. Error bar represents the SE of 3 independent experiments.

Supplementary Table S1 The number of embryos for different genotype is showed at each developmental stage.

	Developmental stages							
Genotype	E12.5	E13.5	E14.5	E15.5	E16.5	E18.5	E19.5	Total
+/+	13	7	36	8	17	16	15	112(23.9)
+/-	26	23	68	32	27	36	26	238(50.9)
-/-	15(27.8)	9(23.1)	28(21.2)	14(25.9)	15(25.4)	13(20.0)	24(36.9)	118(25.2)
Total	54	39	132	54	59	65	65	468

Percentages are in parentheses.

Supplementary Materials and methods

Generation of Jmjd3$^{-/-}$ mice

To investigate the role of JMJD3 in vivo, we generated conditional *Jmjd3* knockout mice with C57BL/6-background by homologous recombination. A targeting vector was designed to replace the exons from 14 to 20, which contain the JmjC H3K27 demethylase domain (Fig. S2A). Candidate of embryonic stem (ES) cells was screened by PCR (Fig. S2B) and further confirmed by Southern blot analysis (Fig. S2C). *Jmjd3*$^{+/-}$ mice were generated by crossing *Jmjd3*$^{+/F}$ mice with the EIIa-cre strain mice (Jackson Labs No.003724). *Jmjd3*$^{-/-}$ embryos were generated by crossing *Jmjd3* heterozygotes. PCR and cDNA sequencing confirmed that the H3K27me3 demethylase domain of Jmjd3 gene were lost in *Jmjd3*$^{-/-}$ mice (Fig.S2D, E). The following primers P1 and P2 were used for the genotyping of *Jmjd3* mutant by PCR on genomic DNAs isolated from the tail biopsies: P1, 5'-GCAGTATAAAACCAGAGGAAACAATG-3' and P2, 5'-GAGGCAGAACC-TGAGCAAGACC-3'. With the two primers, it is possible to amplify specific WT (2355 bp) and mutant (400 bp) DNA fragments (Fig.S2D). Western blot analysis confirmed the absence of JMJD3 in *Jmjd3*$^{-/-}$ cells (Fig.S2F), suggesting that the deletion of the Jmjc domain in vivo may adversely affect protein folding and result in degradation of truncated JMJD3. Immunohistochemistry also indicated that JMJD3 protein lost in *Jmjd3*$^{-/-}$ embryo (Fig.S2G). All animal procedures were conducted in accordance with

the Guidelines for the Care and Use of Laboratory Animals and were approved by the Institutional Animal Care and Use Committee at Shanghai Institutes for Biological Sciences.

Morphological and histology analysis

Whole-mount staining of skeletal preparation by alcian blue and alizarin red was performed as described previously (McLeod, 1980). For histological analyses, mice at various embryonic time points were collected, fixed in 10% formalin, processed, and embedded in paraffin or OCT (Tissue-Tek; Thermo Fisher Scientific). Serial sections were taken at 4 μm thickness and stained with hematoxylin and eosin according to standard techniques. To detect mineral deposition, Von Kossa staining was performed and counterstained by alcian blue and nuclear fast red. Alkaline phosphatase staining and apoptosic detection were performed on 7 μm cryostat sections using alkaline phosphatase kit (Millpore) or in situ cell death detection kit (Roche) following the manufacturer's instructions. Expression of JMJD3 was detected by immunohistochemistry using a polyclonal rabbit anti-mouse primary antibody (Abcam, ab38113), an HRP-conjugated anti-rabbit secondary IgG and a DAB substrate. Hematoxylin was used for counterstaining. For proliferation of chondrocytes by BrdU or KI67 analyses, pregnant females were injected with BrdU as described previously (Wang et al., 2009). BrdU or KI67 positive nuclei were detected by immunohistochemistry with anti-BrdU or anti-KI67 antibodies

(Abcam, ab1893, ab66155) and sections were counterstained with hematoxylin. Cell proliferation rates were determined by counting the percentages of BrdU or KI67 positive cells in total chondrocytes distributed in growth plates. Double-labled immunofluorescences with anti-JMJD3 (Rabbit Polyclonal, Abcam, ab38113), anti-RUNX2 (mouse monoclonal, Abcam, ab76956), anti-Flag (mouse monoclonal, Sigma, F1804) and anti-His (Rabbit Polyclonal, Abcam, ab1187) antibodies were performed on paraffin-embedded sections or the slides of cells according to standard protocols. For in situ hybridization, digoxigenin-11-UTP-labed single-stranded RNA probes were prepared with a DIG RNA labeling kit (Roche) according to the manufacturer's instructions. *Col2a1* and *Col10a1* probes were described (Takeda et al., 2001). *Ihh* cDNA probe was a gift from Brendan Lee (Baylor College of Medicine, Houston). We carried out in situ hybridization as described previously (Kitazawa et al., 1999). Images for skeletons were taken using a stereo microscope (SZX16; Olympus) equipped with a digital camera (DP71; Olympus). Images for double immunofluorescence were captured with a confocal microscope (LAS SP5; Leica) using a 40×/1.25 NA oil objective (Leica) or 63×/1.4 NA oil objective (Leica) at room temperature. All other images were visualized with a microscope (BX51; Olympus) using a 10×, 20 or 40× objectives, and images were captured with the digital camera (DP71; Olympus) using accompanying software. Figures were composed using Adobe Photoshop CS2.

Isolation of limb cartilage tissues and primary chondrocyte culture

Primary mouse limb cartilages and chondrocytes were isolated as described but modified (Gosset et al., 2008). Briefly, E14.5 embryos were sacrificed and genotyped using tail tissues. Whole limbs were treated with 0.05% trypsin (GIBCO) for 30 min at 37℃ and all the soft tissues were eliminated with a Pasteur pipette. The isolated limb cartilage nodules were washed with PBS and then digested in fresh collagenase D (Sigma) solution in Petri dishes in a 37℃ incubator overnight with intermittent shaking. A fresh Pasteur pipette was used to disperse any cell aggregates. Obtained isolated chondrocytes were cultured on a 10cm culture dish in high-glucose Dulbecco's modified Eagle's medium (DMEM) supplemented 10% fetal bovine serum (GIBCO) and antibiotics (penicillin at 100 units/ml, streptomycin at 100ug/ml; GIBCO). The same medium was used for all the derived cultures, and cells were grown at 37°C under 5% CO2.

RNA isolation, reverse transcription, and real-time PCR

Isolated limb cartilages or collected primary chondrocytes from E14.5 embryos were lysed in TRIzol (Invitrogen) for RNA isolation following standard protocol. 1 μg RNA was used for reverse transcription by Maxima First Strand cDNA Synthesis kit (Takara). Real-time PCR was performed on ABI Fast7500 with Maxima SYBR Green qPCR Master Mix (Takara). $2^{-\Delta\Delta Ct}$ method was used for

relative quantification. The primer pairs used were as follows: *Jmjd3*, 5'-CAACTCCATCTGGCTGTTACTG-3' (forward) and 5'-CCTTCTGCAACCA-ATTCCAG-3' (reverse); *Col2a1*, 5'-CCAGGGCTCCAATGATGTAG-3' (forward) and 5'-GCGGGAGGTCTTCTGTGATC-3' (reverse); *Runx2*, 5'- TGACATCCC-CATCCATCCAC-3' (forward) and 5'-AGAAGTCAGAGGTGGCAGTG-3' (reverse); *Col10a1*, 5'-TCCCAGCACCAGAATCTATC-3' (forward) and 5'-GG-CGTTTGGTACCGTTCAGC-3' (reverse); *Ihh*, 5'- GCTCACCCCCAACTAC-AATC-3' (forward) and 5'- CCAGTGAGTTCAGA- CGGTCC-3' (reverse); *Pth1r*, 5'-GACGGCTTCCTTAATGGCTC-3' (forward) and 5'-GCTTCTTGGTCCAT-CTGTCC-3' (reverse); *Atf4,* 5'-CAAACCTTATG-ACCCACCTG-3' (forward) and 5'-ACCTAGTGGCTGCTGTCTTG-3' (reverse); *Sox9,* 5'-CCAGCAAGAA-CAAGCCACAC-3' (forward) and 5'-TCTCGTTCAGCAGCCTCCAG-3' (reverse); *Ctnnb1*, 5'-ATGGCTTGGAATGAGACTGC-3' (forward) and 5'-GCT-CCATCATAGGGTCCATC-3' (reverse); *Mmp13*, 5'-AGACCTTGTGTTTGCA-GAGC-3' (forward) and 5'-GTTTGCCAGTCACCTCTAAG-3' (reverse); *Gapdh,* 5'-CATCACAGCAACACAGAAGACC-3' (forward) and 5'- ACCAGTAAGCTT-GCCATTGAG-3' (reverse).

Plasmids construction

To generate Flag-tagged full-length JMJD3 and its truncated proteins containing either the N-terminus (JMJD3-N, 1–562aa), the middle part (JMJD3-M, 563–1,162aa) or the C-terminus (JMJD3-C, 1,163–1,641aa)

expressing vectors, full-length mouse *Jmjd3* (a gift from Kai Ge, National Institutes of Health, Bethesda, USA) and matched cDNA truncations were inserted into pLVX-3×Flag expressing vectors. To produce the His-Myc-tagged full-length RUNX2 and its truncations containing either the N-terminus (RUNX2-N, 1–108 aa), the middle region (RUNX2-M, 109-258aa) or the C-terminus (RUNX2-C, 259-528 aa) of RUNX2 expressing vectors, full-length mouse *Runx2* and the matched cDNA segments were subcloned into pcDNA3.1-Myc-His expressing vectors. To generate GST fusion proteins, RUNX2-N, RUNX2-M and RUNX2-C were amplified and inserted into pGEX-4T-1 expressing vectors. To produce His-Myc-tagged JMJD3 truncated proteins, JMJD3-N, JMJD3-M, and JMJD3-C was cloned and subcloned into pcDNA3.1-Myc-His expressing vectors. To generate reporter vectors, the promoters regions of mouse *Ihh* (−2074/+185) and *Runx2* (TSS2, −2056/+34) were amplified by PCR using limbs genomic DNA from C57BL/6 mice and inserted into the pGL3-basic vector. shRNA vectors of mouse *Jmjd3* were constructed as previously described (Barradas et al., 2009). All of the constructs were confirmed by sequencing.

Co- immunoprecipitation and GST pull-down assays

For the immunoprecipitation and immunoblotting of the interaction between overexpressed JMJD3 and RUNX2, HEK293T cells were cotransfected with Flag-tagged *Jmjd3* and His-tagged *Runx2* using Lipofectamine 2000

(Invitrogen) according to the manufacturer's manual. 48 h later, cells were harvested and lysed in buffer containing 0.5% Triton X-100,10% glycerol, 50mM Hepes-KOH (pH 7.5), 140 mM NaCl, 0.5 M EDTA, and complete protease inhibitor cocktail (Roche). The lysates were subjected to immunoprecipitation with anti-Flag M2 agarose (Sigma) overnight, followed by Western blotting with anti-Flag (Sigma, F1804) and anti-His (Abcam, ab1187) antibodies.

For the immunoprecipitation and immunoblotting of the interaction between endogenous JMJD3 and RUNX2, The primary chondrocytes from WT E14.5 limbs were grown to confluence on 10×15cm dishs in DMEM with β-glycerophosphate (5mM) and ascorbic acid (50μg/ml) (Day et al., 2005; Temu et al., 2010). The cells were collected and lysed in buffer containing 0.5% Triton X-100, 10% glycerol, 50mM Hepes-KOH (pH 7.5), 140 mM NaCl, 0.5 M EDTA, and complete protease inhibitor cocktail (Roche). Protein lysate (5 mg) was incubated for 6 hours with 3 μg anti-JMJD3 (Abcam, ab85392) or anti-RUNX2 (Cell Signaling, #8486) antibodies followed by incubation 2h with 40 μl protein A/G plus agarose (Santa Cruz Biotechnology.). Immunoprecipitated proteins were detected by Western blotting with the anti-JMJD3 and anti-RUNX2 antibodies.

To detect the domains of JMJD3 responsible for interaction with RUNX2, HEK293T cells were cotransfected with three Flag-tagged truncated *Jmjd3* and His-tagged *Runx2,* or Flag-tagged *Jmjd3* and His-tagged truncated *Runx2,*

using Lipofectamine 2000 (Invitrogen). 48 h later, cells were collected and lysed in buffer containing 0.5% Triton X-100,10% glycerol, 50mM Hepes-KOH (pH 7.5), 140 mM NaCl, 0.5 M EDTA, and complete protease inhibitor cocktail (Roche). The lysates were subjected to immunoprecipitation with anti-His (Abcam, ab1231) or anti-Flag M2 agarose (Sigma) overnight, followed by Western blotting with anti-Flag (Abcam, F1804) and anti-His (Abcam, ab1187) antibodies.

For GST pull-down assay, the RUNX2-GST, RUNX2-N-(1–108 aa)-GST and RUNX2-C (259-528 aa)-GST fusion proteins were produced in *Escherichia coli* BL21. GST fusion proteins were purified with glutathione-Sepharose beads (GE Healthcare). JMJD3-N (1–562aa) and JMJD3-C (1,163–1,641aa) segmentary proteins were produced using an in vitro protein expression kit (TNT® Coupled Reticulocyte Lysate Systems). The interactions were monitored by Western blotting using anti-GST (Abcam, ab3416) or anti-His antibodies.

Chromatin immunoprecipitation (ChIP) and Luciferase Reporter Assays

Primary chondrocytes from E14.5 limbs, ATDC5 chondrocytes and undifferentiated mouse embryonic stem cells (B6/Blu, ATCC® SCRC-1019™) were used for ChIP experiments. The detail procedure was described previously (De Santa et al., 2007; Burgold et al., 2012; Kartikasari et al., 2013; Zhang et al., 2013). Briefly, 1×10^6 cells was cross-linked with 1% formaldehyde

and incubated for 10 min at room temperature. Formaldehyde was deactivated by adding glycine to a final concentration of 125 mM. Cells were lysed using 800 µl lysis buffer consisted of 50mM Tris–HCl pH 8.0, 10mM EDTA, 1% SDS, and complete proteinase inhibitors (Roche) and sonicated into small chromatin fragments with an average size of 400 bp. 3 mg of rabbit anti-JMJD3 (Abcam, ab85392), anti-H3K27me3 (Millipore, #07-449) or anti-RUNX2 (Cell Signaling, #8486S) antibodies were incubated with sonicated chromatin overnight at 4℃. Subsequently 40 µl protein A/G plus agarose (Santa Cruz Biotechnology) was added and incubated for 2h at 4℃ in total volume of 200 µl RIPA buffer containing 10mM Tris–HCl pH 8.0, 140mM NaCl, 1mM EDTA, 1% Triton X-100, 0.1% SDS and complete protease inhibitor cocktail (Roche). After 5× washing with RIPA buffer and 1× with TE buffer, chromatin was eluted, followed by reverse cross-linking at 65℃ overnight. The DNA fragments were then purified using phenol-chloroform extraction and ethanol precipitation. The purified DNA was quantified by Real-time PCR with Maxima SYBR Green qPCR Master Mix (Takara). 2;$^{\Delta\Delta Ct}$ method was used for relative quantification. The primer pairs around of transcriptional start site used were as follows: *Runx2,* 5'-TAACGCCAGTCGGAGCAGC-3' (forward) and 5'-CTCCCCACTTC -ACCCTCAG-3' (reverse); *Ihh*, 5'-CGAGGAGGAGCGAGTGATTC-3' (forward) and 5'-AGAGGGAAGAGCACTGAGCG-3' (reverse); *Gapdh*, 5'-AATGAGGCG -GGTCCAAAGAG-3' (forward) and 5'-ATCCAGTCCTAGCTCAAGGG-3' (reverse).

HEK293T cells were cultured in DMEM media supplemented with 10% fetal bovine serum. For transient transfection assays, HEK293T cells were plated in 48-well plate at 5×10^3/well overnight and were transfected with 100ng pGL3-basic reporter containing *Runx2* or *Ihh* promoters with or without expression plasmids encoding *Runx2* (100ng), *Jmjd3* (100ng) or *Jmjd3*-shRNA (sh-*Jmjd3*) in increasing amounts (50, 100ng) and 10ng *pRL-Renilla* (Promega) mixed with 1μl Lipofectamine 2000 (Invitrogen). Cells were harvested 48 hours after transfection. For luciferase analysis, the cells were lysed according to the manufacturer's instructions for the Dual-Luciferase Reporter assay (Promega). For luciferase analysis in chondrocytes, ATDC5 chondrocytes were plated in 24-well plate at 1×10^4/well overnight and were transiently transfected with a DNA mixture containing 150ng pGL3-basic reporter containing *Runx2* or *Ihh* promoters and 10ng *pRL-Renilla* (Promega) mixed with 1μl Lipofectamine 2000. After culture for 24 h, the cells were infected with or without lentiviral vectors encoding *Runx2*, *Jmjd3* or *Jmjd3*-shRNA (sh-*Jmjd3*) in increasing amounts at an MOI of 10. After 24 hours, cells were harvested for luciferase analysis according to the manufacturer's instructions for the Dual-Luciferase Reporter assay (Promega).

Statistical analyses

All quantitative data are presented as mean ± standard error (SE) with a minimum of three independent samples. Statistical significance is determined

by two-tailed Student’s t-test.

Supplementary References

Barradas, M., Anderton, E., Acosta, J.C., et al. (2009). Histone demethylase JMJD3 contributes to epigenetic control of INK4a/ARF by oncogenic RAS. Genes Dev *23*, 1177-1182.

Burgold, T., Voituron, N., Caganova, M., et al. (2012). The H3K27 demethylase JMJD3 is required for maintenance of the embryonic respiratory neuronal network, neonatal breathing, and survival. Cell Rep *2*, 1244-1258.

Day, T.F., Guo, X., Garrett-Beal, L., et al. (2005). Wnt/beta-catenin signaling in mesenchymal progenitors controls osteoblast and chondrocyte differentiation during vertebrate skeletogenesis. Dev Cell *8*, 739-750.

De Santa, F., Totaro, M.G., Prosperini, E., et al. (2007). The histone H3 lysine-27 demethylase Jmjd3 links inflammation to inhibition of polycomb-mediated gene silencing. Cell *130*, 1083-1094.

Gosset, M., Berenbaum, F., Thirion, S., et al. (2008). Primary culture and phenotyping of murine chondrocytes. Nat Protoc *3*, 1253-1260.

Kartikasari, A.E., Zhou, J.X., Kanji, M.S., et al. (2013). The histone demethylase Jmjd3 sequentially associates with the transcription factors Tbx3 and Eomes to drive endoderm differentiation. EMBO J *32*, 1393-1408.

Kitazawa, S., Kitazawa, R., and Maeda, S. (1999). In situ hybridization with polymerase chain reaction-derived single-stranded DNA probe and S1 nuclease. Histochem Cell Biol *111*, 7-12.

McLeod, M.J. (1980). Differential staining of cartilage and bone in whole mouse fetuses by alcian blue and alizarin red S. Teratology *22*, 299-301.

Takeda, S., Bonnamy, J.P., Owen, M.J., et al. (2001). Continuous expression of Cbfa1 in nonhypertrophic chondrocytes uncovers its ability to induce hypertrophic chondrocyte differentiation and partially rescues Cbfa1-deficient mice. Genes Dev *15*, 467-481.

Temu, T.M., Wu, K.Y., Gruppuso, P.A., et al. (2010). The mechanism of ascorbic acid-induced differentiation of ATDC5 chondrogenic cells. Am J Physiol Endocrinol Metab *299*, E325-334.

Wang, W., Lian, N., Li, L., et al. (2009). Atf4 regulates chondrocyte proliferation and differentiation during endochondral ossification by activating Ihh transcription. Development *136*, 4143-4153.

Zhang, Z., Feng, J., Pan, C., et al. (2013). Atrophin-Rpd3 complex represses Hedgehog signaling by acting as a corepressor of CiR. J Cell Biol *203*, 575-583.